

SPECIAL

Manuel Braz-César · Rui Barros

Optimal control of a plan asymmetric structure using magnetorheological dampers

Received: 29 March 2016 / Accepted: 12 October 2016 / Published online: 22 October 2016
© Springer-Verlag Berlin Heidelberg 2016

Abstract Although building structures can be perceived as a combination of primary frames in two orthogonal directions, they are three-dimensional systems that usually present a very complex dynamic behavior due to irregular geometric configurations, in particular due to plant stiffness or mass eccentricities. This asymmetric geometry results in coupled lateral–torsional motion produced by wind and seismic loading with consequences in the design of lateral and corner columns. A considerable amount of research effort has been devoted to develop structural control systems to reduce the effects of plan asymmetries and to improve the dynamic behavior of these buildings. This paper presents a numerical analysis of a semi-active control system with MR dampers designed to reduce lateral–torsional responses of a plan asymmetric building structure excited by *El Centro* NS earthquake ground motion. A parametric study comprising passive and semi-active control modes is given to demonstrate the effectiveness of the proposed control system with respect to uncontrolled case. The numerical results prove the efficiency of the semi-active control system and its potential use in mitigating coupled lateral–torsional structural responses.

Keywords Structural control · Asymmetric structures · Semi-active control · MR dampers

1 Introduction

Simplified methods for seismic design of buildings are usually based on the lateral motion of the structural system, assuming that it can be modeled by frames in two orthogonal directions. The torsional component can be introduced in the design process using the rigid diaphragm approach in which floor diaphragms are assumed rigid in their own plane to obtain a more accurate representation of the seismic response. However, building structures are complex systems that typically present plan and/or elevation asymmetries as a result of irregular stiffness, strength and/or mass distribution. For instance, plan asymmetries generate correlated plan translations and rotations that lead to an irregular deformation distribution demand among resisting planes namely at the corner columns. As a consequence, there is an increase in force and ductility demand leading to different damage in these elements that generates structural systems with uneven distribution of strength with a large resistant capacity in some load-resisting planes. It should be noted that nowadays, the availability of powerful computational tools has made possible to model complex three-dimensional structures to include combined lateral–torsional motion with high degree of accuracy.

M. Braz-César (✉)
Polytechnic Institute of Bragança, ESTiG, Gab 104, Campus de Santa Apólonia, 5300-253 Bragança, Portugal
E-mail: brazcesar@ipb.pt

R. Barros
Faculty of Engineering of the University of Porto, DEC Rua Dr. Roberto Frias, s/n, 4200-465 Porto, Portugal
E-mail: rcb@fe.up.pt

The complex response of irregular building structures can be significantly attenuated using a wise distribution of the structural elements and/or properties that can be modified through the height of the structure in a stepwise fashion at prescribed story levels. Another possible approach is to use control systems to reduce the effects of coupled lateral–torsional motion due to wind or earthquake loading. In fact, a considerable amount of research effort has been devoted over the last 20 years on developing smart control systems for vibration reduction of structures, in particular simplified structural systems with regular geometry. It has been shown that supplemental energy dissipation systems represent an effective approach to reducing the magnitude of both plan translations and rotations in irregular building structures [1–6]. The performance of these control systems can be considerably improved using active or semi-active actuators which can deal with structural nonlinearities, variations in the dynamic loading and modifications of the properties of structural elements. Among the different vibration control technology available, magnetorheological (MR) fluid-based devices seem to have the suitable features to develop simple, efficient and cost-effective semi-active control systems for vibration mitigation in civil structures. MR fluids are essentially non-colloidal suspensions of micro-sized magnetisable particles in an inert base fluid along with some additives. The yield strength of MR fluids can be directly modified in the presence of a magnetic field making them particularly adequate to develop control devices in which controlled fluid motion is required such as smart dampers. Thus, MR dampers present a variable damping with the ability to transmit force in a controlled manner in accordance with a prescribed magnetic field, improving their energy dissipation performance compared with traditional dampers. This constitutes an important feature to develop enhanced control systems for many engineering applications, such as the dynamic response of both regular and irregular building structures. In this regard, several studies had already been conducted to investigate the effectiveness of these semi-active actuators to control lateral–torsional coupled responses of asymmetric building structures [7–9].

This paper is devoted to evaluate the effectiveness of MR dampers to mitigate the combined lateral–torsional response of a three-dimensional asymmetric-plan structure under seismic excitation.

The numerical formulation and the dynamic behavior of irregular building structures are initially addressed. The principle of operation of a semi-active control system with MR dampers for a two-story, one-bay building structure with one-way asymmetric structural plan under an unidirectional earthquake ground motion is also presented. In this case, two MR dampers installed between the base and the first floor with a symmetric distribution with respect to the earthquake loading direction are used in passive and semi-active control modes. Numerical simulations are carried out to evaluate the effectiveness of MR dampers in mitigating coupled lateral–torsional motions of the asymmetric building structure. The results for the passive and semi-active configurations are compared with those of the uncontrolled case. Finally, the effectiveness of each control mode is analyzed and evaluated emphasizing the main advantages and limitations of each methodology in controlling the response of the irregular structure. This paper is based upon Braz-César and Barros [10], but the current paper has been enhanced, including new performance criteria to better evaluate the effectiveness of the proposed semi-active control system.

2 Numerical formulation

A two-story three-dimensional building structure subjected to a unidirectional seismic excitation will be used to study the performance of a control system with MR dampers. The schematic representation of the model is shown in Fig. 1. In this case, two MR dampers are located at the first floor level, which can be operated in passive and semi-active configurations. The floor diaphragm can be considered rigid in its own plane, and therefore, the dynamic analysis is conducted using a lumped mass model where the whole story mass is lumped at the floor level.

Due to the rigid diaphragm approximation, the response of the structure can be described by three degrees-of-freedom (DOFs) per floor, i.e., two orthogonal translations and a rotation about the vertical axis, resulting in a six DOFs system. Thus, the displacement vector can be expressed as

$$X(t) = \{x_1(t), y_1(t), \theta_1(t), x_2(t), y_2(t), \theta_2(t)\}^T \quad (1)$$

where $x_i(t)$ and $y_i(t)$ denotes the displacements of the center of mass of the i th floor in the x - and y -directions, respectively, and $\theta_i(t)$ is the vector of rotations of the i th floor about the vertical axis. The asymmetric configuration of the two-story structure is obtained by adding an eccentric point mass m_a in both floors as shown in Fig. 2. The resultant system has a symmetric mass distribution on the y -direction and a non-symmetric distribution with respect to the x -axis, which is characterized by the mass eccentricity e_y depicted in Fig. 2.

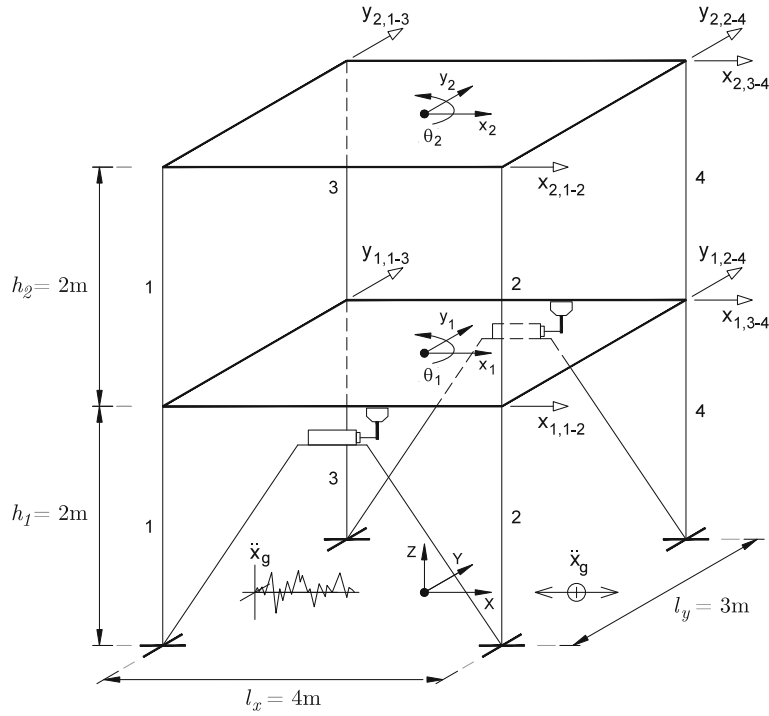


Fig. 1 Two-story building under unidirectional seismic excitation with two MR dampers

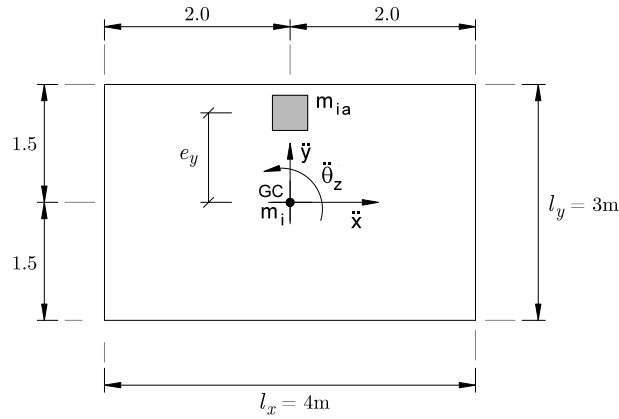


Fig. 2 Floor slab with asymmetric mass distribution

The equation of motion of the building structure subjected to unidirectional earthquake excitation and including the control devices or control forces is given by

$$M\ddot{X}(t) + C\dot{X}(t) + KX(t) = -M\lambda\ddot{x}_g(t) + \Gamma f(t) \quad (2)$$

where M , C and K are the mass, damping and stiffness matrices, respectively. The seismic loading \ddot{x}_g (i.e., in the x -direction) is applied in the structural system using the location vector

$$\lambda = \{1, 0, 0, 1, 0, 0\}^T \quad (3)$$

The force vector describing the two control forces is given by

$$f(t) = \{f_{c,1}(t), f_{c,2}(t)\}^T \quad (4)$$

and the correspondent location matrix can be expressed as

$$\Gamma = \begin{bmatrix} 1 & 1 \\ 0 & 0 \\ l_y/2 & -l_y/2 \\ 0 & 0 \\ 0 & 0 \\ 0 & 0 \end{bmatrix} \quad (5)$$

Since the slab has a rigid body motion, the mass matrix represents a lumped system with two masses with mass eccentricities e_y and $e_x = 0$. Moreover, the additional point mass m_a has a negligible rotational inertia, and therefore, the mass matrix is expressed as

$$M = \begin{bmatrix} m_{1x} + m_{1a} & 0 & -m_{1a}e_y & 0 & 0 & 0 \\ 0 & m_{1y} + m_{1a} & 0 & 0 & 0 & 0 \\ -m_{1a}e_y & 0 & I_1 + m_{1a}e_y^2 & 0 & 0 & 0 \\ 0 & 0 & 0 & m_{2x} + m_{2a} & 0 & -m_{2a}e_y \\ 0 & 0 & 0 & 0 & m_{2y} + m_{2a} & 0 \\ 0 & 0 & 0 & -m_{2a}e_y & 0 & I_2 + m_{2a}e_y^2 \end{bmatrix} \quad (6)$$

where m_i and I_i represent the lumped masses and moments of inertia of the i th floor, respectively (with $i = 1, 2$). The stiffness matrix is expressed in accordance with the displacement vector as

$$K = \begin{bmatrix} K_{x1} + K_{x2} & 0 & 0 & -K_{x2} & 0 & 0 \\ 0 & K_{y1} + K_{y2} & 0 & 0 & -K_{y2} & 0 \\ 0 & 0 & K_{\theta1} + K_{\theta2} & 0 & 0 & -K_{\theta2} \\ -K_{x2} & 0 & 0 & K_{x2} & 0 & 0 \\ 0 & -K_{y2} & 0 & 0 & K_{y2} & 0 \\ 0 & 0 & -K_{\theta2} & 0 & 0 & K_{\theta2} \end{bmatrix} \quad (7)$$

where

$$K_{xi} = \sum_{j=1}^4 k_{xj}, \quad K_{yi} = \sum_{j=1}^4 k_{yj}, \quad K_{\theta i} = \frac{l_y^2}{4} \sum_{j=1}^4 k_{xj} + \frac{l_x^2}{4} \sum_{j=1}^4 k_{yj} \quad \text{for } i = 1, 2 \quad (8)$$

are the stiffness coefficients (the coordinates x_i and y_i can be expressed in terms of the in-plane dimensions of the floor slab l_{xi} and l_{yi} in the x - and y -directions, respectively). The damping matrix can be constructed from the mass and stiffness matrices using the so-called proportional damping, which can be expressed as

$$C = \alpha M + \beta K \quad (9)$$

where α and β are coefficients that can be determined from two vibration modes of the system. The state space equation of the controlled structure can be defined as

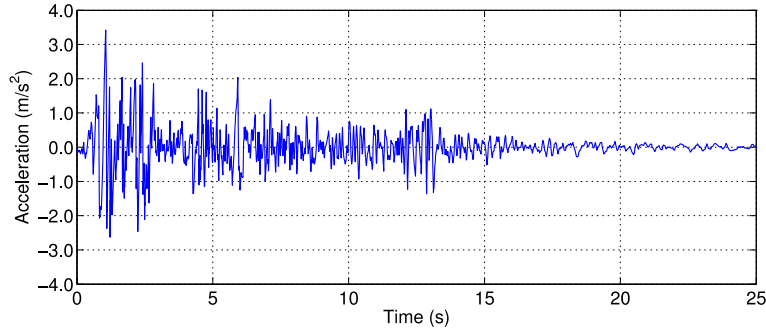
$$\dot{z}(t) = Az(t) + Bf(t) + E\ddot{x}_g(t) \quad (10)$$

where $z(t) = \{X(t), \dot{X}(t)\}^T$ is the state space vector, A is the system matrix, B is an additional matrix accounting for the position of the control forces in the structure, f is a column vector with the control forces (same as Eq. 4) and E is the input vector that accounts for the location of the earthquake loading, which are given by

$$A = \begin{bmatrix} 0 & I \\ -M^{-1}K & -M^{-1}C \end{bmatrix}, \quad B = \begin{bmatrix} 0 \\ M^{-1}\Gamma \end{bmatrix}, \quad E = \begin{bmatrix} 0 \\ -\lambda \end{bmatrix} \quad (11)$$

Table 1 Parameters of the two-story building structure

| Parameter | Value | Parameter | Value |
|---|-----------|---|---------------------------|
| Aspect ratio of the floor slab (l_y/l_x) | 0.75 | Damping ratio for the first and fourth modes (ζ_1, ζ_4) | 2 (%) |
| Lumped mass of the first floor (m_1) | 1750 kg | Polar moment of inertia (first floor), I_1 | 3646 (kg m ²) |
| Lumped mass of the second floor (m_2) | 1750 kg | Polar moment of inertia (second floor), I_2 | 3646 (kg m ²) |
| Lateral stiffness of each column (k_{xj}) | 1050 kN/m | Lateral stiffness of each column, k_{yj} | 355 (kN/m) |

**Fig. 3** Time-scaled El Centro NS earthquake ground motion (0.5t)

The response of the system can be determined using the state space output vector

$$\hat{y}(t) = \hat{C}z(t) + \hat{D}f(t) + \hat{F}\ddot{x}_g(t) \quad (12)$$

where matrices \hat{C} , \hat{D} , and \hat{F} are computed as

$$\hat{C} = \begin{bmatrix} I & 0 \\ 0 & I \\ -M^{-1}K & -M^{-1}C \end{bmatrix}, \quad \hat{D} = \begin{bmatrix} 0 \\ 0 \\ -M^{-1}\Gamma \end{bmatrix}, \quad \hat{F} = \begin{bmatrix} 0 \\ 0 \\ -\lambda \end{bmatrix} \quad (13)$$

when displacements, velocities and accelerations of each floor/mass are being monitored. The output vector can be defined in accordance with the necessary output signals.

3 Case study

The following example presents a numerical analysis of a two-story asymmetric structure under unidirectional seismic loading to investigate the effectiveness of the semi-active control system with two MR dampers located between the base and the first floor. The properties of the lumped mass structure are given in Table 1.

In this case, the asymmetric configuration of the structural system is achieved by adding an eccentric point mass $m_a = 250$ kg in both floors (see Fig. 3). The damping matrix can be constructed in accordance with the formulation presented in Eq. 9, in which $\alpha = 0.476685$ and $\beta = 0.000671$.

The N-S component of the *El Centro* 1940 ground motion (peak acceleration of 3.42 m/s²) will be used as the unidirectional seismic excitation. The mass and stiffness properties were defined in such a way that the building structure represents a reduced scale model (1:2). Thus, the earthquake time history was scaled in time by a factor of 0.5 to characterize the magnitude of displacements that would be observed in experiments tests. In this case, the time was scaled to 20% of the full-scale earthquake time history as displayed in Fig. 3.

A numerical model of a small-size commercial MR fluid damper RD-1005-3 manufactured by LORD Corporation is used in this study. This MR damper has been widely studied to design semi-active control systems for a wide variety of engineering applications and also to investigate and derive numerical models for this type of devices. The nonlinear hysteretic behavior of MR dampers can be modeled by parametric and nonparametric models. A well-known parametric model is the modified Bouc–Wen model illustrated in Fig. 4.

According to the mechanical arrangement depicted in Fig. 4, the predicted damper force F_{MR} produced by the MR damper can be computed from

$$F_{MR} = \rho s + c'_0(\dot{x}' - \dot{y}') + k'_0(x' - y') + k'_1(x' - x'_0) = c'_1\dot{y}' + k'_1(x' - x'_0) \quad (14)$$

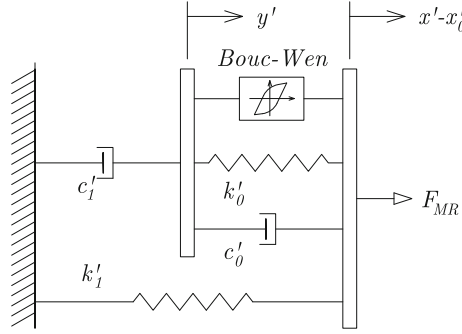


Fig. 4 Modified Bouc–Wen or Spencer model [11]

in which

$$\dot{y}' = \frac{1}{c'_0 + c'_1} [\rho s + c'_0 \dot{x}' + k'_0(x' - y')] \quad (15)$$

is dependent on the evolutionary variable

$$\dot{s} = \delta \dot{x}' - \zeta |\dot{x}'| s |\dot{s}|^{n-1} - \gamma \dot{x}' |s|^n \quad (16)$$

In this formulation, k'_1 and c'_0 are the accumulator stiffness and the viscous damping observed at larger velocities, respectively. The parameter c'_1 is used to produce the roll-off that is observed in the experimental data at low velocities, k'_0 is used to control the stiffness at large velocities and x'_0 is the initial displacement associated with the nominal damper force f_0 due to the accumulator. Parameters ζ , γ , δ and n are used to control the linearity in the unloading and the smoothness of the transition from the pre-yield to the post-yield region. Some of the modified Bouc–Wen parameters can be described by constant values, i.e., they are current-independent parameters. To take into account the influence of the magnetic field, parameters ρ , c'_0 and c'_1 are usually defined as a linear function of the current, i.e., they are current-dependent parameters described by

$$\rho(u) = \rho_a + \rho_b u \quad (17)$$

$$c'_0(u) = c'_{0a} + c'_{0b} u \quad (18)$$

$$c'_1(u) = c'_{1a} + c'_{1b} u \quad (19)$$

Besides, to accommodate the dynamics involved in the MR fluid reaching rheological equilibrium, the following first-order filter is used

$$\dot{u} = -\eta(u - v) \quad (20)$$

in which the applied current u is described with a time delay relative to the desired current v and η is the time constant of the first-order filter. The model parameters of a RD-1005-03 MR damper were identified based on experimental data [12]. The current-independent parameters are: $\delta = 10.013$, $\zeta = 3.044 \text{ mm}^{-2}$, $\gamma = 0.103 \text{ mm}^{-2}$, $k'_0 = 1.121 \text{ N/mm}$, $f_0 = 40 \text{ N}$ (related to x'_0) and $n = 2$ (pre-defined parameter). It was found that the current-dependent parameters can be described by polynomial functions as follows

$$\rho(u) = -826.67u^3 + 905.14u^2 + 412.52u + 38.24 \text{ [N/mm]} \quad (21)$$

$$c'_0(u) = -11.73u^3 + 10.51u^2 + 11.02u + 0.59 \text{ [N s/mm]} \quad (22)$$

$$c'_1(u) = -54.40u^3 + 57.03u^2 + 64.57u + 4.73 \text{ [N s/mm]} \quad (23)$$

and finally, the first-order filter is described by $\eta = 140 \text{ s}^{-1}$.

A set of numerical simulations was carried out to determine the responses of the two-story asymmetric system. Initially, the response of the uncontrolled structure was obtained from Eq. 10 by setting $f_c = 0$ (i.e., no control forces). The response of the uncontrolled system will be used as the reference signal to evaluate the performance of the passive and semi-active control systems. A new numerical simulation was carried out to obtain the responses of the structure using the MR dampers in a passive OFF mode (zero current input) and passive ON mode (maximum value of the operating current). In this case, the actuators act on the first floor/mass

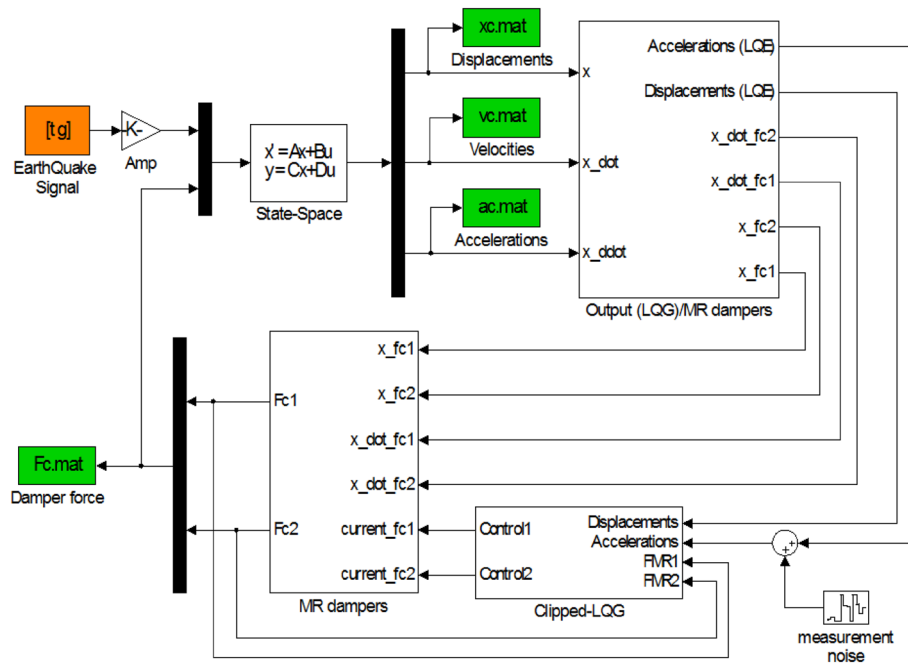


Fig. 5 Block diagram of the clipped-optimal LQG controller

in a passive control mode (i.e., as passive energy dissipation devices) producing two passive control forces f_{c1} and f_{c2} along the x -direction. Finally, the MR dampers are used as semi-active actuators in combination with a traditional optimal LQG controller. Each control mode is intended to reduce the coupled lateral–torsional response of the structural system.

All the simulations were carried out in MATLAB/Simulink. The block diagram of the semi-active LQG control system for the two-story building structure is shown in Fig. 5. The controller uses floor accelerations and displacements across the dampers to compute the control signal. Indeed, a semi-active control strategy based on acceleration feedback seems to be more reliable for structural control applications instead of full-state feedback or velocity feedback controllers.

The clipped-optimal (CO) algorithm represents a traditional semi-active control strategy for MR dampers. This classical controller has proved capable of exploring in a very efficient manner the potential of these semi-active actuators, in particular the variable damping force. The main objective of the semi-active controller for MR dampers is to append n force feedback loops to induce each device to produce approximately a desired control force [13–16]. In order to do this, the control strategy combines two controllers:

- A primary controller that includes an optimal control unit which is responsible for determining the optimal or desired control forces of an ideal active control system that should be applied to the structure to reduce the system response;
- A secondary controller or bistate selector (clipping system). Since only the current/voltage applied to the current driver of the MR damper can be directly controlled, this controller has the function to generate the corresponding control signal in the form of a bistate control output by clipping the optimal control forces. This accounts for the nonlinear nature of MR dampers, ensuring that they only produce dissipative forces (i.e., by adapting the ideal control action to the semi-active nature of the actuator).

In this case, the primary controller uses a linear quadratic Gaussian (LQG) regulator to compute the optimal control forces. The LQG controller combines a linear quadratic regulator (LQR) with a Kalman filter or linear quadratic estimator (LQE). The Kalman filter is used to reconstruct the state vector based on a few output measurements of a noisy system, and then, the LQR component is used to compute the optimal input signal based on the estimated state vector. The observer gain L must be adjusted to achieve the required performance. A high gain allows the filter to follow the observations more closely, while a low gain follows the predictions more closely. This is accomplished by setting

$$Q_w = q_w I_e, \quad R_v = r_v I_m \quad (24)$$

where I_e and I_m are identity matrices related to the number of excitation inputs and measurement signals, respectively. Finally, the LQG controller is a combination of a Kalman filter (or a LQE) with a linear quadratic regulator (LQR), i.e.,

$$\begin{aligned}\dot{\hat{x}} &= (A - L\hat{C})\hat{x} + B\hat{u} + L\hat{y} \\ \hat{u} &= -G\hat{x}\end{aligned}\quad (25)$$

where G and L are the LQR and LQE gain matrices, respectively, that need to be adjusted to obtain the desired control action. The solution is based on the separation principle in which the full-state feedback controller (i.e., the LQR) and the Kalman filter are designed independently and then combined to form the LQG compensator.

The selection of Q_w and R_v depends on the level of accuracy attributed to the model and the measurements. For an accurate system model measured with poor sensors, one should probably select Q_w to be larger than R_v , while for a poorly modeled system with accurate measurements, one should probably choose R_v to be larger than Q_w . A common approach is to set one of the tuning parameters and adjust the other parameter until the result is satisfying. The key is to have a Kalman filter that removes as much noise as possible without being too slow to adapt to changes.

The secondary controller is used to convert the control forces estimated by the primary controller into a bistate control signal (bang–bang/on–off controller) to command the MR actuators. The damping forces generated by the MR dampers are dependent on the local responses of the structural system, and therefore, the devices cannot always produce the desired optimal control forces. Consequently, only the control voltage/current can be directly controlled to change the damper force and a force feedback loop is then incorporated in the control algorithm to make the MR damper to generate approximately the desired optimal control force. To achieve this objective, the following command signal algorithm is applied

$$F_{MR} = \begin{cases} f_c, & f_c \cdot \dot{x}' < 0 \\ 0, & \text{otherwise} \end{cases} \quad (26)$$

When the MR damper is delivering the desired optimal force, the operating voltage/current should remain the same. If the magnitude of the damper force is smaller than the magnitude of the desired optimal force and the two forces have the same sign, the voltage/current applied to the current driver is increased to the maximum level. Otherwise, the commanded voltage is set to zero. The algorithm for selecting the command signal for the i th MR damper can be stated as

$$v_i = V_{\max} H[(f_{ci} - f_i) f_i] \quad (27)$$

where V_{\max} is the saturation voltage/current of the MR damper, f_{ci} is the desired optimal control force, f_i is the measured damper force and H is the Heaviside step function.

Hence, the clipped-optimal LQG control algorithm is a semi-active controller that combines a LQG method with a bistate selection unit. The linear optimal controller is used to compute the desired control force f based on the measured structural responses y and control force vector f applied to the structure through the semi-active device. Next, a secondary controller comprising a clipping unit generates a bistate control signal based on the optimal force calculated by the first controller so that it can be adapted to the dissipative nature of the MR damper allowing this actuator to generate approximately the desired control force [13–16]. To illustrate the application of the type of control scheme, in the present example it is assumed that acceleration measurements and displacement across the dampers are the only state variables available to design the optimal controller. A probable location of the accelerometers is depicted in Fig. 6.

The translational and rotational response of the asymmetric structure is described by four accelerometers on each floor, two on the x -direction and two on the y -direction, with a total of eight accelerometers. Additionally, two displacement sensors (e.g., two LVDTs) are used to measure the displacements across the two dampers, which represent the displacement of each corner of the first floor slab in the x -direction. These sensor measurements define the output response vector

$$\hat{y} = \{x_{1,1}, x_{1,2}, \ddot{x}_{1,1}, \ddot{x}_{1,2}, \ddot{y}_{1,1}, \ddot{y}_{1,2}, \ddot{x}_{2,1}, \ddot{x}_{2,2}, \ddot{y}_{2,1}, \ddot{y}_{2,2}\}^T \quad (28)$$

The Kalman gain L is calculating by adjusting Q_w and R_v . It is assumed that each sensor has identically distributed and statistical independent Gaussian white noise and therefore the covariance between the measurement noise and the process noise. Since the measurement noise is equal and independent for all outputs, R_v is a diagonal matrix. Then, Q_w is tuned through q_w until the LQE output is adequate. Likewise, the weighting

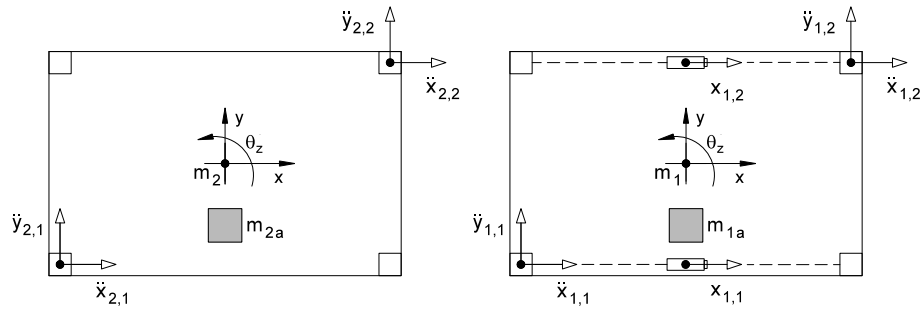


Fig. 6 Location of the measurement sensors in each floor (Eight accelerometers and two LVDTs)

Table 2 Peak responses under the time-scaled El Centro earthquake (0.5t)

| Control strategy | x (cm) | \dot{x} (cm/s) | \ddot{x} (cm/s ²) | θ (rad) | $\dot{\theta}$ (rad/s) | $\ddot{\theta}$ (rad/s ²) | drift (cm) | $\Delta\theta/h$ (rad) | f (N) |
|------------------|--------------|------------------|---------------------------------|----------------|------------------------|---------------------------------------|--------------|------------------------|-------------|
| Uncontrolled | 1.005 | 28.30 | 813 | 8.6e-4 | 0.028 | 0.901 | 1.005 | 8.6e-4 | — |
| | 1.652 | 42.76 | 1211 | 1.4e-3 | 0.041 | 1.395 | 0.658 | 5.2e-4 | — |
| Passive | 0.933 | 25.61 | 728 | 7.6e-4 | 0.024 | 0.805 | 0.933 | 7.6e-4 | 213 |
| OFF | 1.523 | 39.40 | 1100 | 1.2e-3 | 0.036 | 1.227 | 0.603 | 4.6e-4 | 183 |
| Passive | 0.540 | 15.03 | 462 | 3.8e-4 | 0.0125 | 0.513 | 0.540 | 3.8e-4 | 1546 |
| ON | 0.857 | 24.43 | 837 | 6.3e-4 | 0.0199 | 0.691 | 0.367 | 2.5e-4 | 1459 |
| Clipped-Optimal | 0.527 | 13.55 | 531 | 3.3e-4 | 0.0119 | 0.524 | 0.528 | 3.3e-4 | 1421 |
| LQG controller | 0.819 | 23.77 | 729 | 6.0e-4 | 0.0191 | 0.738 | 0.346 | 2.7e-4 | 1416 |

The first and second lines represent the peak responses for the first and second floors, respectively (first and second MR dampers in the case of the damper force). Passive OFF represents zero current input, and passive ON represents the maximum operating current

matrices Q and r of the LQR controller must be adjusted in order to determine the state gain matrix G . In the present case, different configurations of the weighting matrix Q and the control parameter r were evaluated by measuring the effect of each combination in the system response. The following weighting parameters provided the best results in reducing the structural responses of the asymmetric system

$$Q = \begin{bmatrix} K & 0 \\ 0 & 0 \end{bmatrix}; \quad R = r \begin{bmatrix} 1 & 0 \\ 0 & 1 \end{bmatrix}; \quad r = 2 \times 10^{-5} \quad (29)$$

It is important to note that the performance of the optimal controller is dependent on the selection of the weighting matrices. Thus, the results attained with the proposed LQG controller could be further improved by optimizing the weighting parameters with advanced search/optimization tools or soft computing techniques such as genetic algorithms or neural networks.

4 Results

A comparison of the peak responses of each control mode to those of the uncontrolled system is summarized in Table 2 (numbers in bold indicate reference and lower values). The results show the effectiveness of the proposed semi-active control system in reducing the coupled lateral-torsional response of the three-dimensional structure. In this case, the semi-active system outperforms the passive control modes in almost all peak responses (with exception of the angular acceleration, although with a significant reduction compared with the uncontrolled case). The results also show that using the MR dampers in a semi-active configuration results in lower peak drifts compared with the passive ON configuration. Regarding the passive control mode, it can be seen that the passive OFF configuration has almost a reduced effect in the system response (around 10%). The passive ON mode has a major effect in the system response that results in peak responses being significantly reduced especially the torsional motions (around 55%). As to be expected, the maximum passive control action is achieved by keeping the MR damper permanently switched on, which is clearly observable in the results of the numerical analysis.

In general, the LQG controller is able to reduce both translational and torsional responses of the asymmetric structure, offering significant performance gains in controlling the torsional motion of the floor decks. Although in some cases the passive configuration performed slightly better than the semi-active system, the latter present

Table 3 Evaluation criteria for the structural responses (peak ratios)

| Evaluation criterion | Description |
|--|--|
| $J_1 = \max_{t,i} \left(\frac{ \dot{x}_{i,c}(t) }{ \dot{x}_{\max,u}(t) } \right)$ | Maximum peak floor displacement ratio whereby the floor displacements over time are normalized by the maximum peak uncontrolled displacement |
| $J_2 = \max_{t,i} \left(\frac{ \ddot{x}_{i,c}(t) }{ \ddot{x}_{\max,u}(t) } \right)$ | Maximum peak floor velocity ratio whereby the floor velocities over time are normalized by the maximum peak uncontrolled velocity |
| $J_3 = \max_{t,i} \left(\frac{ \ddot{\theta}_{i,c}(t) }{ \ddot{\theta}_{\max,u}(t) } \right)$ | Maximum peak floor acceleration ratio whereby the floor accelerations over time are normalized by the maximum peak uncontrolled acceleration |
| $J_4 = \max_{t,i} \left(\frac{ \dot{\theta}_{i,c}(t) }{ \dot{\theta}_{\max,u}(t) } \right)$ | Maximum peak floor rotation ratio whereby the floor rotations over time are normalized by the maximum peak uncontrolled rotation |
| $J_5 = \max_{t,i} \left(\frac{ \ddot{\theta}_{i,c}(t) }{ \ddot{\theta}_{\max,u}(t) } \right)$ | Maximum peak floor angular velocity ratio whereby the floor angular velocities over time are normalized by the maximum peak uncontrolled angular velocity |
| $J_6 = \max_{t,i} \left(\frac{ \ddot{\theta}_{i,c}(t) }{ \ddot{\theta}_{\max,u}(t) } \right)$ | Maximum peak floor angular acceleration ratio whereby the floor angular accelerations over time are normalized by the maximum peak uncontrolled angular acceleration |

Subscript $i = 1, 2$ denotes the story index and subscripts c and u represent controlled and uncontrolled cases

Table 4 Evaluation criteria for the structural responses (RMS ratios)

| Evaluation criterion | Description |
|---|--|
| $J_7 = \max_{t,i} \left(\frac{\ \dot{x}_{i,c}(t)\ }{\ \dot{x}_{\max,u}(t)\ } \right)$ | Maximum RMS floor displacement ratio, which is given in terms of the maximum RMS absolute displacement over time with respect to the uncontrolled case |
| $J_8 = \max_{t,i} \left(\frac{\ \ddot{x}_{i,c}(t)\ }{\ \ddot{x}_{\max,u}(t)\ } \right)$ | Maximum RMS floor velocity ratio, which is given in terms of the maximum RMS absolute velocity over time with respect to the uncontrolled case |
| $J_9 = \max_{t,i} \left(\frac{\ \ddot{\theta}_{i,c}(t)\ }{\ \ddot{\theta}_{\max,u}(t)\ } \right)$ | Maximum RMS floor acceleration ratio, which is given in terms of the maximum RMS absolute acceleration over time with respect to the uncontrolled case |
| $J_{10} = \max_{t,i} \left(\frac{\ \dot{\theta}_{i,c}(t)\ }{\ \dot{\theta}_{\max,u}(t)\ } \right)$ | Maximum RMS floor rotation ratio, which is given in terms of the maximum RMS absolute rotation over time with respect to the uncontrolled case |
| $J_{11} = \max_{t,i} \left(\frac{\ \ddot{\theta}_{i,c}(t)\ }{\ \ddot{\theta}_{\max,u}(t)\ } \right)$ | Maximum RMS floor angular velocity ratio, which is given in terms of the maximum RMS absolute angular velocity over time with respect to the uncontrolled case |
| $J_{12} = \max_{t,i} \left(\frac{\ \ddot{\theta}_{i,c}(t)\ }{\ \ddot{\theta}_{\max,u}(t)\ } \right)$ | Maximum RMS floor angular acceleration ratio, which is given in terms of the maximum RMS absolute angular acceleration over time with respect to the uncontrolled case |
| $J_{13} = \max_{t,i} \left(\frac{\ d_{i,c}(t)\ }{\ d_{\max,u}(t)\ } \right)$ | Maximum RMS inter-story drift ratio, which is given in terms of the maximum RMS absolute inter-story drift over time with respect to the uncontrolled case. Inter-story drift $d_i = \delta_i / h_i$ |

Subscript $i = 1, 2$ denotes the story index and subscripts c and u represent controlled and uncontrolled cases

overall the best performance. The proposed controller presents a performance improvement in reducing the peak responses exhibiting the best overall performance when compared with the passive configurations. The maximum ratios of the peak responses attained with this controller are generally smaller than that of passive ON configuration, with the significant exception of the angular acceleration of the second floor. Besides, the peak control force achieved by the clipped-optimal LQG algorithm has the lowest value (1416 kN).

Next, a new set of evaluation criteria including normalized and RMS responses and also control requirements was used to complete the performance assessment of each control mode. The first six criteria (J_1 to J_6) are based on the peak responses as shown in Table 3.

The next six criteria (J_7 to J_{13}) are related to the RMS structural responses (see Table 4). In these equations, $\|\cdot\|$ denotes the absolute value and $\|\cdot\|$ is the L_2 norm given by

$$\|\cdot\| = \sqrt{\frac{1}{t_f} \int_0^{t_f} [\cdot]^2 dt} \quad (30)$$

where $t_f = t_{\max}$ represents the total excitation duration and t_f represents a sufficient large time to allow the response to attenuate. Finally, the last three performance indices (J_{14} to J_{16}) are intended to evaluate the effectiveness of the MR dampers (Table 5).

Table 5 Evaluation criteria for the MR dampers (actuators)

| Evaluation criterion | Description |
|--|--|
| $J_{14} = \max_{t,j} \left(\frac{ f_j(t) }{W} \right)$ | Maximum control force generated during the control action normalized by the weight of the structure (where W represents the total weight of the structure) |
| $J_{15} = \max_{t,j} \left(\frac{\sum_j P_j(t)}{\dot{x}_{\max} \cdot W} \right)$ | Maximum control power normalized by $(\dot{x}_{\max} \cdot W)$, i.e., the uncontrolled velocity times the weight of the structure |
| $J_{16} = \max_{t,j} \left(\frac{\sum_j \frac{1}{t_f} \int_0^{t_f} P_j(t)}{\dot{x}_{\max} \cdot W} \right)$ | Total power required to control the response of the structure normalized by $(\dot{x}_{\max} \cdot W)$ with actuator index $j=2$ |

Table 6 Results of the evaluation criteria for each control strategy

| Evaluation criteria | | Passive control | | |
|---------------------|----------|-----------------|---------------|---------------|
| | | Passive OFF | Passive ON | CO-LQG |
| Peak responses | J_1 | 0.922 (78 %) | 0.519 | 0.496 (−4 %) |
| | J_2 | 0.921 (61 %) | 0.571 | 0.556 (−3 %) |
| | J_3 | 0.908 (31 %) | 0.691 | 0.602 (−13 %) |
| | J_4 | 0.892 (94 %) | 0.459 | 0.441 (−4 %) |
| | J_5 | 0.877 (80 %) | 0.488 | 0.468 (−4 %) |
| | J_6 | 0.879 (77 %) | 0.496 | 0.529 (7 %) |
| RMS responses | J_7 | 0.861 (127 %) | 0.380 | 0.386 (2 %) |
| | J_8 | 0.859 (131 %) | 0.372 | 0.377 (1 %) |
| | J_9 | 0.862 (116 %) | 0.400 | 0.412 (3 %) |
| | J_{10} | 0.855 (146 %) | 0.347 | 0.339 (−2 %) |
| | J_{11} | 0.852 (142 %) | 0.352 | 0.356 (1 %) |
| | J_{12} | 0.849 (125 %) | 0.378 | 0.433 (15 %) |
| | J_{13} | 0.860 (132 %) | 0.371 | 0.383 (3 %) |
| | J_{14} | 5.4e−3 (−86 %) | 0.039 | 0.038 (−3 %) |
| Control | J_{15} | 6.0e−3 (−78 %) | 0.027 | 0.024 (−11 %) |
| | J_{16} | 1.1e−3 (−58 %) | 2.6e−3 | 2.4e−3 (−8 %) |

Values under parenthesis are the percentage of reduction with respect to the passive ON case

The results achieved for each control configuration are presented in Table 6. It should be noted that small values of the evaluation criteria are generally more desirable and indicate a better performance of the control system under analysis. Thus, the results highlight the effectiveness of the semi-active systems in reducing peak responses but also reveal the low performance of the proposed controllers with respect to the RMS values of the system responses in comparison with best passive control configuration.

As can be seen, the overall performance of the clipped-optimal LQG controller outperforms the passive ON mode showing a significant peak response reduction in the translational displacement of the second floor (up to 13 % compared with the passive ON mode). On the other hand, the normalized peak inter-story rotation is higher than that achieved with the best passive configuration. Regarding the RMS responses, the performance of the semi-active controller is not as good as the passive ON configuration. However, the performance obtained with the clipped-optimal LQG has almost the same RMS values of the best passive control mode (in some cases, it is slightly better than the passive system, e.g., J_{10}). In addition to the peak responses reduction, what stands out in this study is the improvement in power requirements of the control system when the semi-active controller is used to command the MR dampers. The proposed semi-active controller shows an important decrease in the total power required to control the response of the structure (in this case is around 8 %). Hence, the semi-active operation of this type of actuators offers improved power efficiency while producing a better peak response reduction than that of the passive modes.

5 Conclusions

This paper has presented a numerical analysis of a semi-active control system to reduce coupled lateral–torsional response of an asymmetric building structure using MR dampers. The performance of the control system was evaluated by comparing the responses due to *El Centro* earthquake excitation for passive and

semi-active configurations with the corresponding uncontrolled response. It was verified that the proposed semi-active optimal controller allows a more efficient management of the actuators presenting in general a better performance than the passive control modes. Hence, it can be concluded that the semi-active control system outperforms a fully passive system allowing a considerable reduction in combined lateral and torsional motion of the three-dimensional plan asymmetric structure using only two MR dampers in a non-collocated configuration. Further research must be carried out to validate the application of these MR damper-based control systems to a wide range of structural configurations and with different semi-active controllers.

References

1. Jangid, R.S., Datta, T.K.: Performance of multiple tuned mass dampers system for torsionally coupled system. *Earthq. Eng. Struct. Dyn.* **26**, 307–317 (1997)
2. Goel, R.K.: Effects of supplemental viscous damping on seismic response of asymmetric-plan systems. *Earthq. Eng. Struct. Dyn.* **27**(2), 125–141 (1998)
3. Lin, W.H., Chopra, A.K.: Understanding and predicting effects of supplemental damping on seismic response of asymmetric one-storey system. *Earthq. Eng. Struct. Dyn.* **30**, 1475–1494 (2001)
4. García, M., Llera, J.C., Almazan, J.L.: Torsional balance of plan asymmetric structures with viscoelastic dampers. *Eng. Struct.* **29**, 914–932 (2007)
5. Mevada, S.V., Jangid, R.S.: Seismic response of asymmetric systems with linear and non-linear viscous dampers. *Int. J. Adv. Struct. Eng.* **4**(5), 1–20 (2012)
6. Joshi, J.H., Mevada, S.V., Patel, S.B.: Response of two-way asymmetric system with linear and non linear viscous dampers under bi-directional earthquake. *Int. J. Innov. Eng. Technol.* **2**(2), 92–102 (2013)
7. Yoshida, O., Dyke, S.J.: Response control of full-scale irregular buildings using magnetorheological dampers. *J. Struct. Eng.* **131**(5), 734–742 (2005)
8. Yoshida, O., Dyke, S.J., Giacosa, L.M., Truman, K.Z.: Experimental verification on torsional response control of asymmetric buildings using MR dampers. *Earthq. Eng. Struct. Dyn.* **32**, 2085–2105 (2003)
9. Bharti, S.D., Shriali M.K.: Seismic Response Control of Asymmetric Plan Building with Semiactive MR Damper, 15 WCEE, Portugal (2012)
10. Braz-Cesar, M., Barros, R.: Vibration control of asymmetric structures using MR dampers, 13th Conference on Dynamical Systems Theory and Applications DSTA 2015, Dynamical Systems: Control and Stability, vol. **3**, pp. 107–118 (2015)
11. Spencer Jr., B.F., Dyke, S.J., Sain, M.K., Carlson, J.D.: Phenomenological model for magnetorheological dampers. *J. Eng. Mech.* **123**(3), 230–238 (1997)
12. Braz-César, M.: Vibration Control of Building Structures Using MR dampers, Ph.D. thesis, Faculty of Engineering of the University of Porto (2015)
13. Dyke, S.J., Spencer, B.F., Sain, M.K., Carlson, J.D.: Seismic response reduction using magnetorheological dampers. *Proceedings of the IFAC World Congress, USA*, pp. 145–150 (1996)
14. Dyke, S.J., Spencer, B.F., Sain, M.K., Carlson, J.D.: Modeling and control of magnetorheological dampers for seismic response reduction. *Smart Mater. Struct.* **5**, 565–575 (1996)
15. Dyke, S.J., Spencer, B.F.: A comparison of semi-active control strategies for the MR damper. *IASTED International Conference on Intelligent Information Systems. IEEE Computer Society*, pp. 580–584 (1997)
16. Dyke, S.J., Spencer, B.F., Sain, M.K., Carlson, J.D.: Experimental Verification of Semi-Active Structural Control Strategies Using Acceleration Feedback. *Proceedings of the 3rd International Conference on Motion and Vibration Control*, vol. **3**, pp. 291–296 (1996)